Title
Insertion of the CXC chemokine ligand 9 (CXCL9) into the mouse hepatitis virus genome results in protection from viral-induced encephalitis and hepatitis.

Journal
Virology, 382(2)

ISSN
1096-0341

Authors
Muse, Michael
Kane, Joy AC
Carr, Daniel JJ
et al.

Publication Date
2008-12-01

DOI
10.1016/j.virol.2008.09.032

Peer reviewed

Since January 2020 Elsevier has created a COVID-19 resource centre with free information in English and Mandarin on the novel coronavirus COVID-19. The COVID-19 resource centre is hosted on Elsevier Connect, the company's public news and information website.

Virology 382 (2008) 132–144

Contents lists available at ScienceDirect

Virology

journal homepage: www.elsevier.com/locate/yviro

Insertion of the CXC chemokine ligand 9 (CXCL9) into the mouse hepatitis virus genome results in protection from viral-induced encephalitis and hepatitis ☆

Michael Muse [a], Joy A.C. Kane [a], Daniel J.J. Carr [b], Joshua M. Farber [c], Thomas E. Lane [a,d,*]

[a] Department of Molecular Biology and Biochemistry, University of California, Irvine 92619-3900, USA
[b] Department of Ophthalmology, University of Oklahoma Health Sciences Center, Oklahoma City, OK 73104, USA
[c] Inflammation Biology Section, Laboratory of Molecular Immunology, National Institutes of Health, Bethesda, MD 20892, USA
[d] Center for Immunology, University of California, Irvine, CA 92619-3900, USA

ARTICLE INFO

Article history:
Received 14 February 2008
Returned to author for revision
17 March 2008
Accepted 23 September 2008
Available online 29 October 2008

Keywords:
Chemokines
Virus
Central nervous system
Host defense

ABSTRACT

The role of the CXC chemokine ligand 9 (CXCL9) in host defense following infection with mouse hepatitis virus (MHV) was determined. Inoculation of the central nervous system (CNS) of *CXCL9*−/− mice with MHV resulted in accelerated and increased mortality compared to wild type mice supporting an important role for CXCL9 in anti-viral defense. In addition, infection of *RAG1*−/− or *CXCL9*−/− mice with a recombinant MHV expressing CXCL9 (MHV-CXCL9) resulted in protection from disease that correlated with reduced viral titers within the brain and NK cell-mediated protection in the liver. Survival in MHV-CXCL9-infected *CXCL9*−/− mice was associated with reduced viral burden within the brain that coincided with increased T cell infiltration. Similarly, viral clearance from the livers of MHV-CXCL9-infected mice was accelerated but independent of increased T cell or NK cell infiltration. These observations indicate that CXCL9 promotes protection from coronavirus-induced neurological and liver disease.

Introduction

Inoculation of mouse hepatitis virus (MHV, a positive-strand RNA virus) into the central nervous system (CNS) of susceptible mice results in an acute encephalomyelitis that is characterized by widespread viral replication primarily in astrocytes, microglia, and oligodendrocytes (reviewed in Bergmann et al., 2006; Glass et al., 2002). Chemokines are expressed within the CNS early following MHV infection and are important in host defense by attracting activated lymphocytes bearing the appropriate chemokine receptor which then participate in reduction in viral burden via secretion of IFN-γ and cytolytic activity (Chen et al., 2001; Liu et al., 2000, 2001a; Parra et al., 1999, 2000). However, viral RNA/antigen often persists and surviving mice will develop an immune-mediated demyelinating disease with similar clinical and histologic characteristics to the human demyelinating disease multiple sclerosis (MS) (Lane and Buchmeier, 1997; Marten et al., 2001; Templeton and Perlman, 2007; Weiner, 1973). Secretion of chemokines during chronic disease amplifies the severity of demyelination in MHV-infected mice by recruiting activated T cells and macrophages into the CNS that participate in myelin destruction (Glass et al., 2004; Liu et al., 2001b).

Early following MHV infection, the CXC chemokine ligand 10 (CXCL10, also known as IP-10) is expressed primarily by ependymal cells, astrocytes, and microglia (Lane et al., 1998). CXCL10 aids in defense during acute disease by attracting antigen-specific T cells expressing the receptor CXCR3. Indeed, use of blocking antibodies specific for either CXCL10, CXCR3, or infection of CXCL10 deficient mice results in impaired T cell trafficking into the CNS of MHV-infected mice and delayed viral clearance (Dufour et al., 2002; Liu et al., 2000; Stiles et al., 2006). Moreover, CXCL10 expression is also important in enhancing innate immune responses by attracting NK cells into the CNS which aid in defense through the secretion of IFN-γ (Trifilo et al., 2004). CXCL9 (also known as MIG, monokine induced by interferon gamma) is a CXC chemokine that is closely related to CXCL10 with regards to both structure and function (Farber, 1997). Similar to CXCL10, CXCL9 is expressed by a wide variety of cell types following exposure to cytokines including IFN-α/β and IFN-γ (Farber, 1997; Ho and Ivashkiv, 2006). In addition, CXCL9 expression is correlated with host defense following infection of mice with poxvirus (Mahalingam et al., 1999, 2000), murine cytomegalovirus (Hokeness et al., 2007; Salazar-Mather et al., 2000), adenovirus (Arai et al., 2002) and transgenic mice capable of replicating hepatitis B virus (Kakimi et al., 2001a, 2001b) by attracting CXCR3-expressing T cells and NK cells to sites of viral infection and replication. With regards to MHV infection, blocking CXCL9 function by administering anti-CXCL9 antibodies to infected mice resulted in increased mortality and enhanced recovery of virus from the brain that correlated

☆ This work was supported by National Institutes of Health grants NS41249 (T.E.L.) AI067309 (D.J.J.C.) and National Multiple Sclerosis Society Grant 3278-A-3 to T.E.L.

* Corresponding author. Department of Molecular Biology and Biochemistry 3205 McGaugh Hall University of California, Irvine Irvine, CA 92619-3900, USA. Fax: +1 949 824 8551.
E-mail address: tlane@uci.edu (T.E. Lane).

0042-6822/$ – see front matter © 2008 Elsevier Inc. All rights reserved.
doi:10.1016/j.virol.2008.09.032

with reduced T cell infiltration (Liu et al., 2001). Together, these findings emphasize an important role for both CXCL9 and CXCL10 in orchestrating the recruitment of targeted CXCR3+lymphocytes into the CNS in response to MHV infection that aid in host defense by reducing viral burden.

The current study was undertaken to further our understanding of how the chemokine CXCL9 participates in innate immune responses following MHV infection of the brain and liver as earlier studies from our laboratory support an important role for chemokines in shaping host defense in the absence of an adaptive immune response (Trifilo et al., 2004). In addition, the ability of mice deficient in CXCL9 (*CXCL9*−/− mice) to generate an effective host response in response to MHV infection was determined. To accomplish these goals, we infected mice in which CXCL9 expression was genetically silenced (*CXCL9*−/− mice) with a recombinant MHV that expresses CXCL9 (MHV-CXCL9) from a dispensable open reading frame within the viral genome and infected *RAG1*−/− and *CXCL9*−/− mice to evaluate how CXCL9 contributes to anti-viral defenses following MHV infection of the brain and liver.

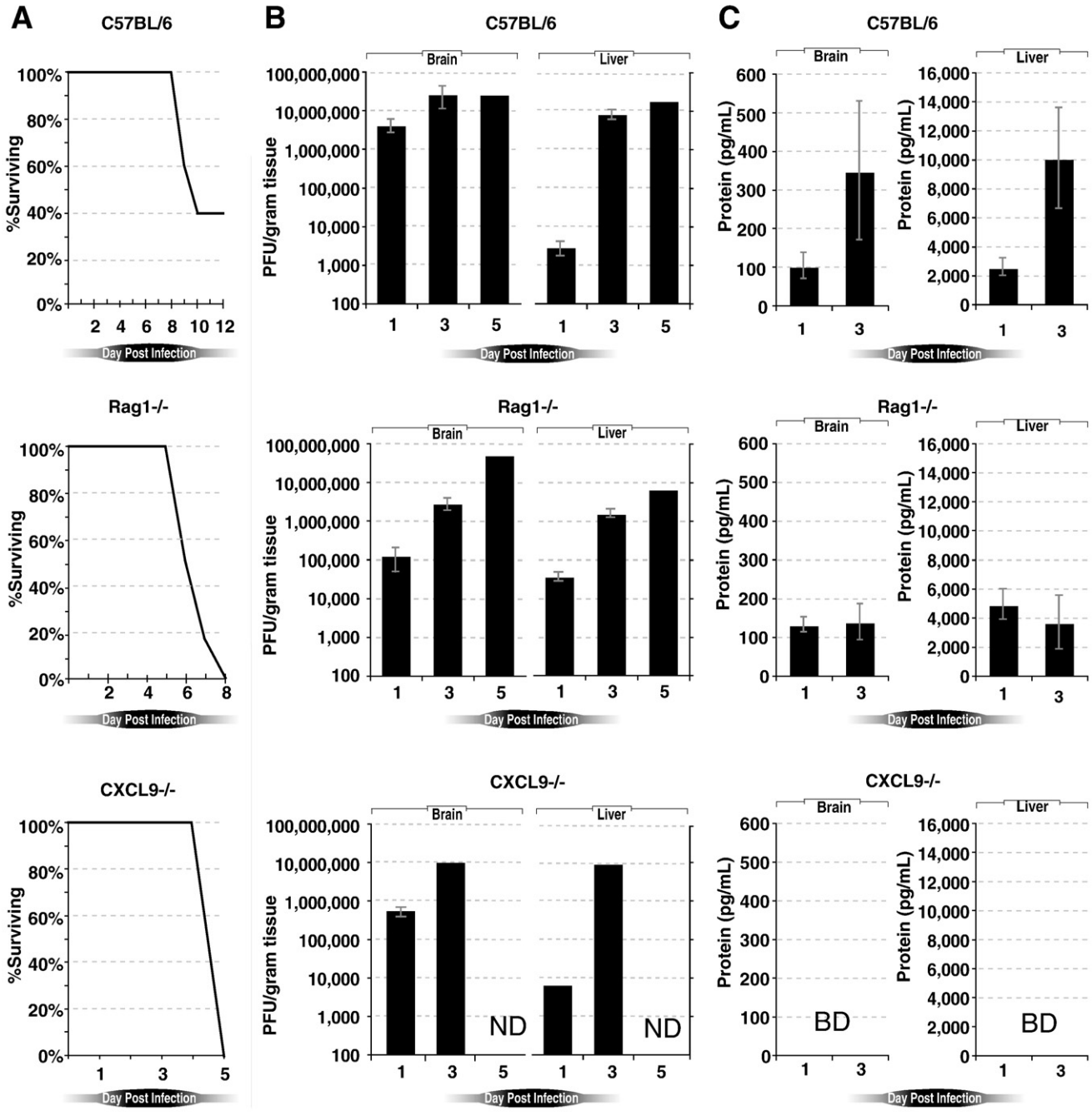

Fig. 1. CXCL9 is important in host defense following coronavirus infection. C57BL/6 (*CXCL9*+/+), *RAG1*−/−, and *CXCL9*−/− mice were i.c. infected with 5000 PFU of MHV-A59 and survival, viral titers, and CXCL9 production determined. (A) Both *CXCL9*−/− and *RAG1*−/− mice exhibited increased mortality following MHV-A59 infection compared to wild type mice. Data shown are representative of two independent experiments with a minimum of 4 mice per experimental group. (B) Viral titers within the brains and livers were determined at days 1, 3, and 5 p.i. with virus. Similar titers were present within the brains and livers of experimental mice at days 1 and 3 p.i. while by day 5 p.i. there were elevated titers within the brains of *RAG1*−/− mice compared to wild type mice (not significant). Viral titers in brains and livers of infected *CXCL9*−/− mice were not determined (ND) at day 5 due to the high mortality rate. (C) CXCL9 protein levels within brains and livers of infected wild type and *RAG1*−/− mice were determined by ELISA at days 1 and 3 p.i. CXCL9 was below detection (BD) within the brains or livers of sham-infected or infected *CXCL9*−/− mice at days 1 and 3 p.i. Data in B and C are presented as average±SEM and represent two independent experiments with a minimum of three mice per time point.

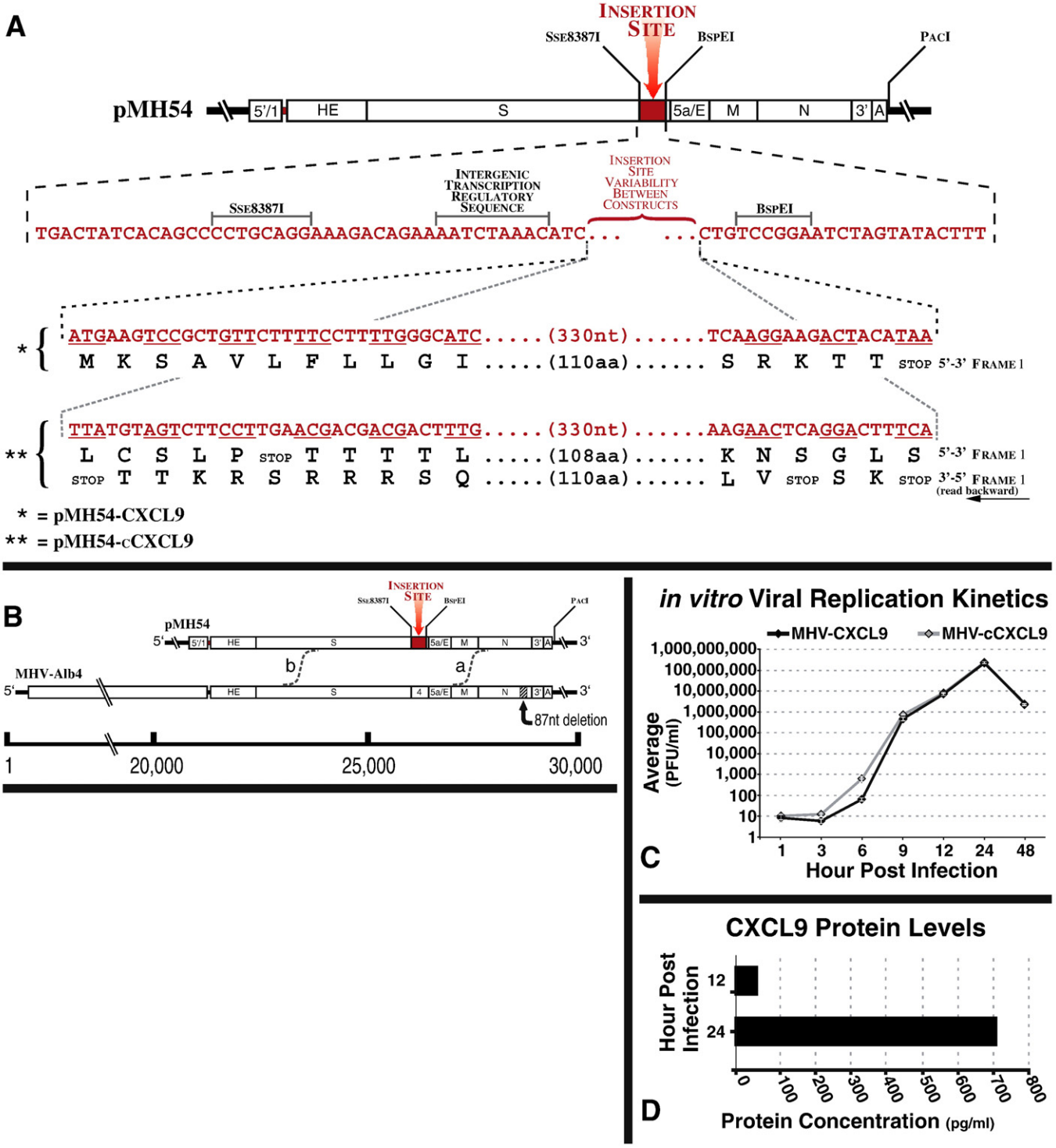

Fig. 2. Construction of a CXCL9-expressing recombinant of MHV-A59. (A) Construction of a transcription vector for synthesis of donor RNA. Plasmids pCXCL9A and pCXCL9B were derived in two steps from parent plasmid pMH54 via intermediate constructs (not shown) resulting in the removal of 267 nucleotides (nt) of MHV sequence from pMH54 and replacement with either CXCL9 sequence in pCXCL9A or inverted CXCL9 sequence in pCXCL9B. Restriction sites shown are those relevant to plasmid construction, runoff *in vitro* transcription, or recombinant analysis. The expanded region of the sequence shows the context of either the inserted CXCL9 ORF or the inverted CXCL9 containing several stop codon sequences. (B) Generation of recombinant viruses. Diagramatic scheme for generation of MHV-A59 CXCL9 or cCXCL9 recombinants by targeted recombination between the parental virus, thermolabile *N* gene deletion mutant *Alb*4, and donor RNA transcribed from either plasmid pCXCL9A or pCXC9B. Recombination events occurring 5′ to the *N* gene yet 3′ to gene for (denoted by "a") will result in generation of WT MHV-A59 genome and will be visualized by large plaques during the screening procedure but fail genetic screening. Recombination events occurring in the region denoted by "b" will result in reconstitution of MHV containing either CXCL9 or cCXCL9 coding sequence. (C) Recombinant virus growth kinetics. Confluent monolayers of 17Cl1 cells were infected with either MHV-CXCL9 (black line) or MHV-cCXCL9 (grey line) at a multiplicity of 0.01 per cell. At the indicated times p.i., aliquots of medium were removed and plaque titers determined on mouse L2 cells. Data shown are a representative experiment from three separate experiments. (D) CXCL9 ELISA analysis. ELISA analysis of CXCL9 protein expression from supernatants of infected cells was performed at indicated time points. No CXCL9 protein was detected in supernatants obtained from cell monolayers infected with MHV-cCXCL9. Results presented are representative of two separate experiments.

Results

MHV infection of CXCL9−/− and RAG1−/− mice

To determine the importance of CXCL9 in host defense following MHV infection, *CXCL9−/−* mice were infected with MHV-A59 and survival compared to infected wild type C57BL/6 (*CXCL9+/+*) and *RAG1−/−* mice. As shown in Fig. 1A, infection of wild type mice with MHV-A59 resulted in ~40% survival by day 12 p.i. In contrast, MHV-A59 infection of *CXCL9−/−* mice resulted in increased susceptibility with 100% of mice dead by day 5 p.i. (Fig. 1A). Similarly, *RAG1−/−* mice infected with virus also exhibited increased susceptibility with 100% of mice dying by day 8 (Fig. 1A). Comparison of viral titers within the brains and livers of infected mice revealed similar titers at days 1 and 3 p.i. (Fig. 1B). Although there were increased viral titers within the brains, but not livers, of *RAG1−/−* at day 5 p.i. compared to wild type mice, this difference was not significant (Fig. 1B). CXCL9 protein was detected within the brains and livers of infected wild type mice and *RAG1−/−* mice at days 1 and 3 p.i. with greater levels present in wild type mice at both times points (Fig. 1C). No CXCL9 protein was detected within tissues of infected *CXCL9−/−* mice (Fig. 1C). These data demonstrate the importance of CXCL9 in host defense following MHV infection of the brain and liver. Presumably, this is the result of deficient recruitment of cells expressing the CXCL9 receptor CXCR3 *e.g.* T cells and NK cells into infected tissues that aid in control of viral replication. Moreover, these data highlight the importance of an adaptive immune response in controlling MHV replication, particularly within the brain, as *RAG1−/−* mice also exhibited increased mortality compared to immunocompetent wild type mice.

Construction and characterization of recombinant viruses

In order to assess the functional contributions of CXCL9 in host defense following MHV infection, we constructed a recombinant of MHV capable of expressing CXCL9 with the goal of instilling this virus into the CNS of either *RAG1−/−* mice or *CXCL9−/−* mice and evaluating disease severity. We inserted the exogenous *CXCL9* gene into a functional transcription unit in the genome of MHV-A59 in place of

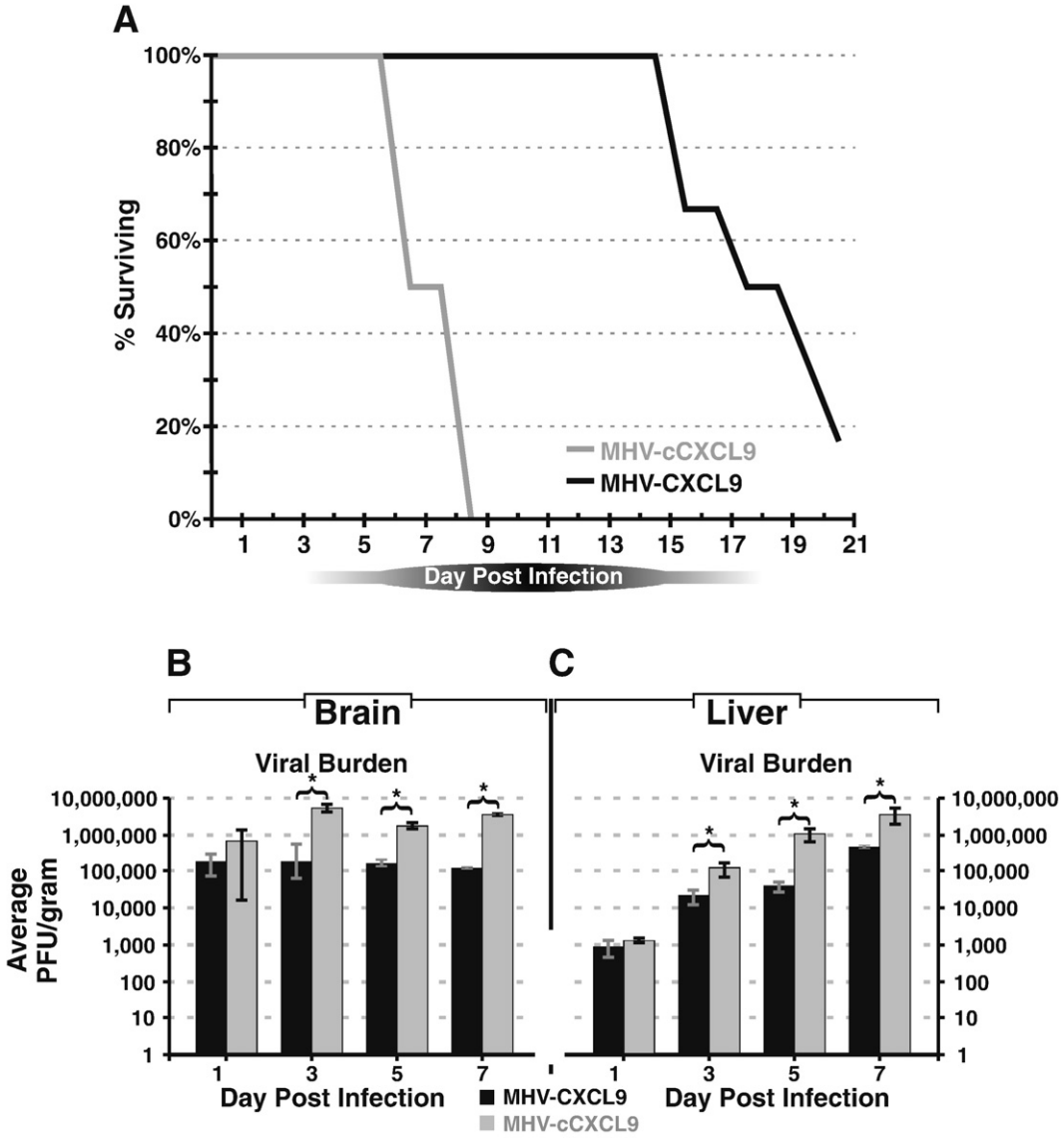

Fig. 3. *RAG1−/−* mortality following infection. (A) Morality curves for *RAG1−/−* mice infected i.c. with either 5000 PFU of MHV-CXCL9 or MHV-cCXCL9. Mice infected with MHV-cCXCL9 exhibited dramatically higher mortality rates with 100% of infected mice dead by day 9 p.i. while ~20% of MHV-CXCL9-infected mice remained alive until day 20 p.i. Data are representative of two separate experiments with a minimum of 6 mice per experimental group. Viral titers are reduced (*$p \leq 0.05$) in the brains (B) and livers (C) of *RAG1−/−* mice infected with MHV-CXCL9 compared to mice infected with MHV-cCXCL9 at days 3, 5, and 7 p.i. Data are presented as the average±SEM and are representative of two separate experiments with a minimum of 4 mice per experimental group.

most of gene 4. *MHV* gene 4 encodes a nonstructural protein that is not essential for replication either in tissue culture or in the mouse host (Ontiveros et al., 2001; Weiss et al., 1993; Yokomori and Lai, 1991). This has been most clearly shown in the JHM strain of MHV, where targeted disruption of both transcription and translation of gene 4 was demonstrated to have no detectable effect on growth in tissue culture or virulence in the mouse CNS (Ontiveros et al., 2001). Moreover, in MHV-A59 the expression of gene 4 is abrogated by a frameshift mutation that truncates the protein after 19 codons (Weiss et al., 1993). The CXCL9-expressing recombinant of MHV was generated by targeted RNA recombination, a reverse genetic system that has been used to manipulate the 31-kb RNA genome of MHV (Koetzner et al., 1992; Masters et al., 1994). To construct recombinants, the CXCL9 ORF was first introduced into plasmid pMH54 (pMH54-CXCL9) downstream of the gene 4 transcription-regulating sequence (TRS) and replacing the first two-thirds of gene 4 (Fig. 2A). As a control, a separate pMH54 vector was generated that contained an inverted CXCL9 ORF (pMH54-cCXCL9) with several engineered stop codons to ensure that generation of a polypeptide was inhibited (Fig. 2A). Viral recombinants were generated through RNA-RNA recombination between either pCXCL9A or pCXCL9B-derived synthetic transcripts and the genome of the *N* gene deletion mutant *Alb*4 (Fig. 2B), which was selected against on the basis of its thermolability (Koetzner et al., 1992; Masters et al., 1994). Independent, plaque-

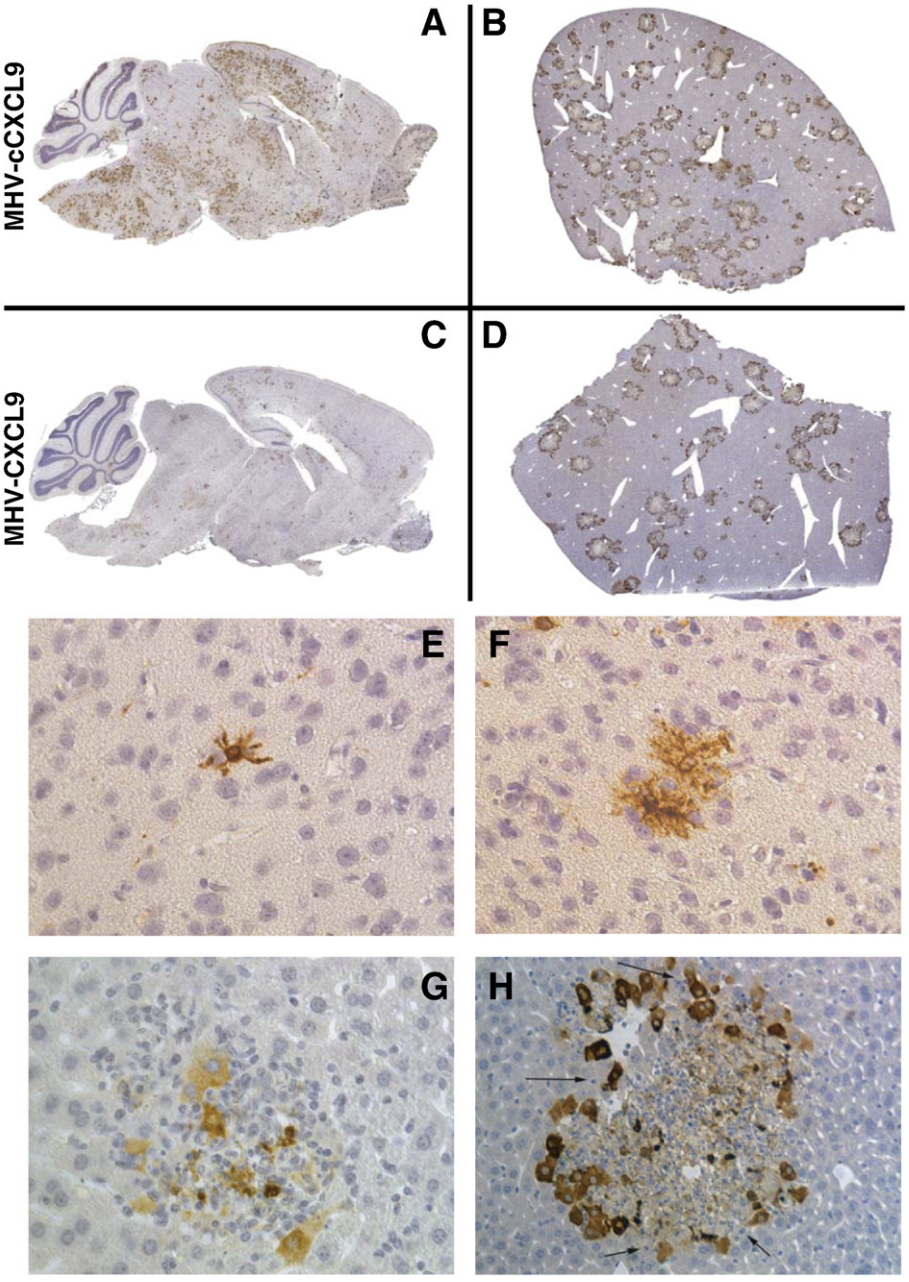

Fig. 4. Viral infection of brain and liver in *RAG1*−/− mice. Representative sagittal sections from brains and livers of mice stained for viral antigen (brown chromagen) from mice infected with either MHV-cCXCL9 (A and B) or MHV-CXCL9 (C and D). MHV-CXCL9 infection results in reduced staining for viral antigen in the brain (C) compared to MHV-cCXCL9-infected mice at day 5 p.i. (A). However, comparison of viral antigen localization between infections displayed similar patterns of infection with staining detected in the hippocampus, thalamus, hypothalamus, and medulla. Moreover, there was no apparent difference in cellular tropism as viral antigen is readily detected in glial cells within the brains of mice infected with either MHV-CXCL9 (E) or MHV-cCXCL9 (F). Brains are representative of 4 mice per group with a minimum of 6 sections/mouse examined. Diminished staining for viral antigen was detected in the livers of MHV-CXCL9-infected mice (D) compared to MHV-cCXCL9-infected mice (B) at day 5 p.i. Viral antigen was detectable within hepatocytes encircling areas of necrotic and focally apoptotic cells (indicated by arrows) that were readily present in MHV-cCXCL9-infected mice (H) yet relatively absent in MHV-CXCL9-infected mice (G). Immunostaining for viral antigen within livers was performed for two separate experiments with a minimum of 2 mice per group with 6 sections per mouse examined.

purified recombinant candidates were characterized by RT-PCR analysis of viral RNA, and the integrity of the CXCL9 ORF or the control CXCL9 (cCXCL9) were ascertained by direct sequencing of purified PCR products. One CXCL9 recombinant virus (MHV-CXCL9) and a control CXCL9 (MHV-cCXCL9) were chosen for subsequent experiments in mice. Both MHV-CXCL9 and MHV-cCXCL9 formed plaques of indistinguishable size and morphology in tissue culture, and both viruses grew to high titers, producing comparable amounts of syncytia and cytopathic effect in infected cells. To directly compare the two recombinants, we separately infected monolayers with either MHV-CXCL9 or MHV-cCXCL9 and determined the infectious titer of virus released at various times from 2 to 48 h p.i. This revealed that the growth kinetics of the CXCL9 recombinant and the control counterpart were indistinguishable (Fig. 2C). To ascertain whether CXCL9 was capable of being secreted by the engineered recombinant virus, supernatants from mock-infected cells or from cells infected with either MHV-CXCL9 or MHV-cCXCL9 were analyzed by ELISA. The results shown in Fig. 2D reveal increased expression of CXCL9 protein at 12 and 24 h from MHV-CXCL9-infected cultures. No CXCL9 was detected within supernatants of cultures following infection with MHV-cCXCL9 (sensitivity of assay < 10 pg/mL).

Intracerebral inoculation of RAG1−/− mice with recombinant viruses

We next determined if *RAG1−/−* mice were protected from disease following infection with MHV-CXCL9. As shown in Fig. 3A, *RAG1−/−* mice infected with MHV-cCXCL9 resulted in death as early as 5 days p.i. and 100% mortality by day 9 p.i. In contrast, MHV-CXCL9-infected mice displayed 100% survival up to 14 days p.i. following infection and ~20% of mice survived until 20 days p.i. Correlating with the increased mortality in mice infected with MHV-cCXCL9, there was a significant increase ($p \leq 0.05$) in viral titers within the brains at days 3, 5, and 7 p.i. as compared to MHV-CXCL9-infected mice (Fig. 3B). In addition, viral titers were reduced within the livers of MHV-CXCL9-infected mice compared to MHV-cCXCL9-infected mice at days 3, 5, and 7 p.i. (Fig. 3C). The enhanced ability to control viral replication within both the brain and livers of MHV-CXCL9-infected mice was not the result of increased IFN-γ secretion as there were no differences in IFN-γ protein levels within the brains as determined by ELISA nor increased expression of MHC class II staining on microglia (data not shown). Immunohistochemical staining supported titer data from brains and livers demonstrating that diminished survival was associated with increased viral antigen within the brain (Fig. 4A) and liver (Fig. 4B) of mice infected with MHV-cCXCL9 as compared to tissues isolated from MHV-CXCL9-infected (Figs. 4C, D). Within the CNS, there were no differences in cellular tropism as viral antigen was detected within glial cells present in mice infected with MHV-CXCL9 (Fig. 4E) and MHV-cCXCL9 (Fig. 4F). Histologic examination of the livers at day 7 p.i. revealed that *RAG1−/−* mice infected with MHV-cCXCL9 contained numerous lesions characteristic of MHV-induced hepatitis characterized by large confluent areas of hepatocyte necrosis with varying degrees of anisonuleosis and multinucleation as well as apoptosis (Fig. 4H). In general, livers from *RAG1 −/−* mice infected with MHV-CXCL9 exhibited fewer and, in general, smaller lesions and less hepatic damage and reactive nucleomegaly (Fig. 4G).

NK cells are protective in response to MHV infection of the liver

CXCL9 has previously been shown to be chemotactic for NK cells expressing CXCR3 (Arai et al., 2002; Kakimi et al., 2001a; Mahalingam et al., 1999). To determine if the decrease in mortality and viral burden reflected differences in the profile of NK cell infiltration, flow cytometric analysis of mononuclear cells isolated from the brains and livers of mice infected with either MHV-CXCL9 or MHV-cCXCL9 was performed. The results shown in Fig. 5A reveal similar levels of NK cells infiltrating into the brains of mice infected with either MHV-

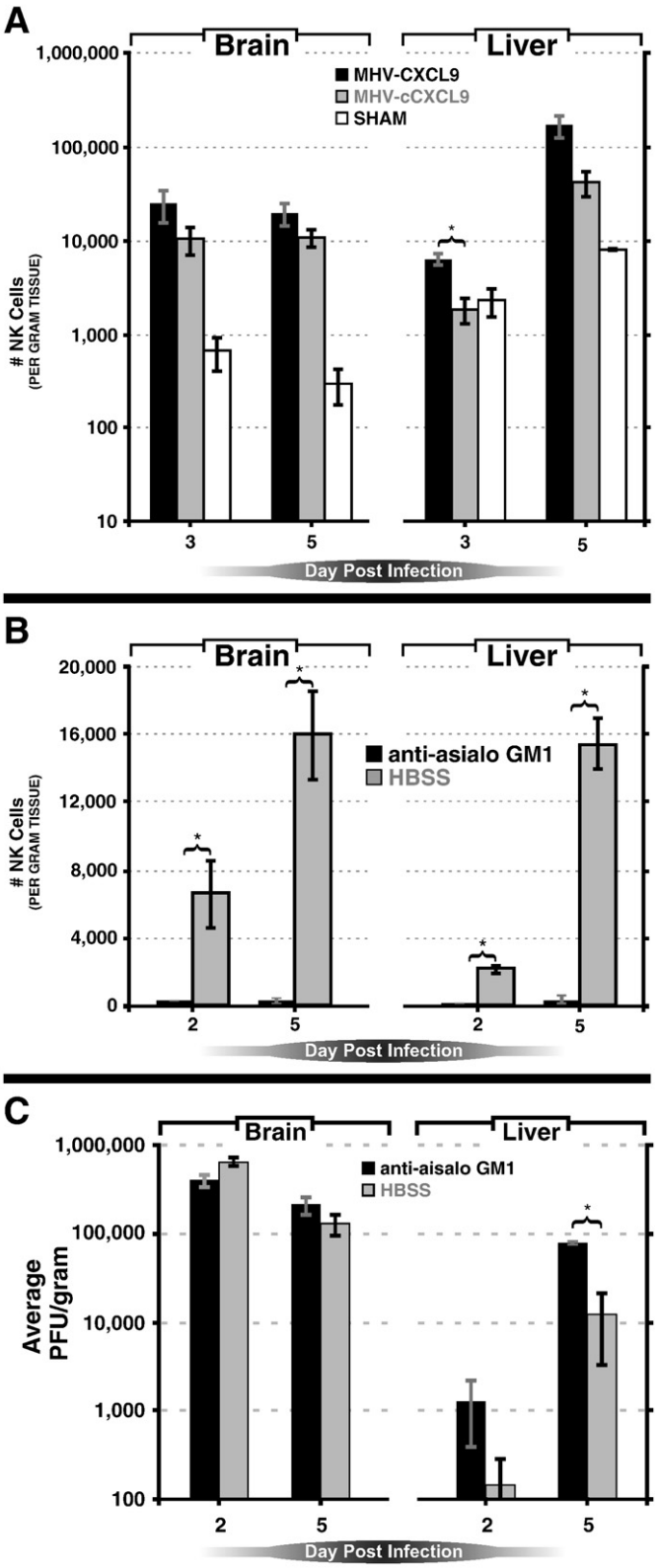

Fig. 5. NK cell infiltration into brains and livers. (A) Total numbers of NK cells (NK1.1+) infiltrating into the brains and livers of *RAG1−/−* mice infected with either MHV-CXCL9 or MHV-cCXCL9. NK cells were elevated ($*p \leq 0.05$) in the livers of mice infected with MHV-CXCL9 at day 3 p.i. compared to MHV-cCXCL9-infected mice. (B) *RAG1−/−* mice were infected with MHV-CXCL9 and treated with anti-asialo GM1 antisera to deplete NK cells. Such treatment resulted in a significant reduction ($*p \leq 0.05$) of NK cells within the brains and livers of infected mice at days 2 and 5 p.i. (C) Depletion of NK cells did not affect viral titers within the brain but resulted in increased viral titers ($*p \leq 0.05$) within the livers at days 2 and 5 p.i. Results are presented as average ± SEM and represent two separate experiments with a minimum of three mice per time point.

CXCL9 or MHV-cCXCL9 at all time points examined indicating that viral-derived CXCL9 did not enhance accumulation of NK cells. NK cell infiltration was increased ($p \leq 0.05$) within livers of MHV-CXCL9-infected mice compared to MHV-cCXCL9 at day 3 p.i. and levels remained elevated by day 5 p.i., although this difference was not significant (Fig. 5A). To further evaluate whether NK cells contributed to host defense, NK cells were depleted from MHV-CXCL9-infected mice through treatment with anti-asialo GM1 antisera (Trifilo et al., 2004) that resulted in a significant reduction ($p \leq 0.001$) in NK cells present in both brain and liver (Fig. 5B). The absence of NK cells within the livers, but not the brain, resulted in a significant ($p \leq 0.01$) increase in viral titers supporting earlier studies indicating that NK cells are important in controlling viral replication in within the livers of MHV-infected mice (Fig. 5C) (Walsh et al., 2007).

Infection of either CXCL9+/+ or CXCL9−/− mice with MHV-CXCL9 results in protection from disease

We next infected wild type C57BL/6 (*CXCL9+/+*) mice with either MHV-CXCL9 or MHV-cCXCL9 in order to assess the contributions of virally-derived CXCL9 to host defense. As shown in Fig. 6A, infection of wild type mice with MHV-cCXCL9 resulted in ~80% survival of mice out to day 21 p.i. while 100% of mice infected with MHV-CXCL9 survived the infection. Correspondingly, enhanced survival in MHV-

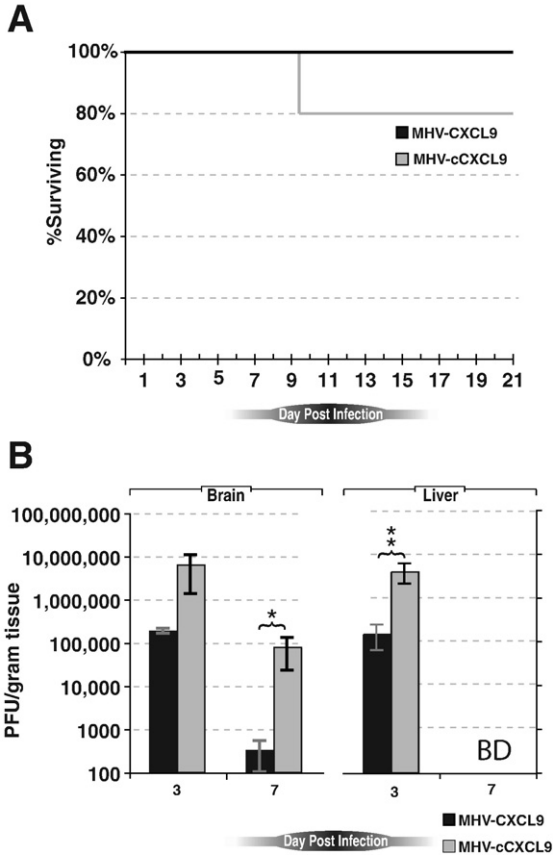

Fig. 6. Viral infection of wild type (*CXCL9+/+*) mice. (A) Morality curves for (*CXCL9+/+*) mice infected i.c. with 5000 PFU of MHV-CXCL9 or MHV-cCXCL9. Infection with MHV-CXCL9 ($n=6$) resulted in 100% survival out to day 21 p.i. and 80% survival in MHV-cCXCL9-infected mice ($n=6$). (B) Viral titers are reduced within the brains of MHV-CXCL9-infected mice at days 3 ($p \leq 0.09$) and 7 p.i. ($p \leq 0.003$) compared to MHV-cCXCL9-infected mice. By day 12 p.i., mice infected with either virus had cleared viral titers below level of detection (~100 PFU/g tissue, not shown). Within the livers, mice infected with MHV-CXCL9 had reduced viral titers ($p \leq 0.01$) compared to MHV-cCXCL9-infected mice at day 3 p.i. yet mice infected with either virus had cleared virus below the level of detection (BD) by day 7 p.i. Data are presented as average±SEM and represent two independent experiments with a minimum of 3 mice per time point.

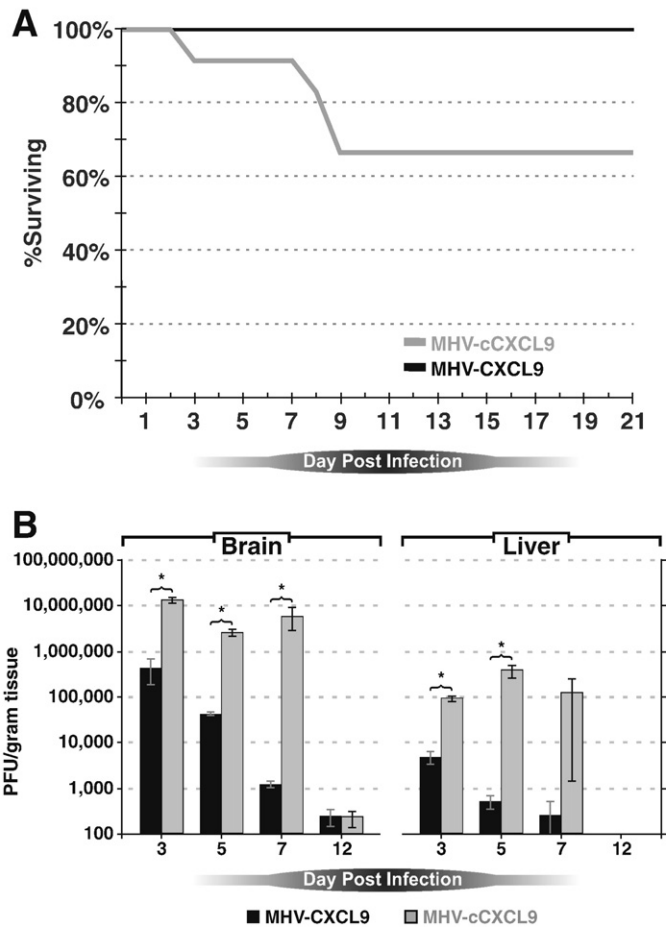

Fig. 7. Viral infection of *CXCL9*−/− mice. (A) Morality curves for *CXCL9*−/− mice infected i.c. with either 5000 PFU of MHV-CXCL9 or MHV-cCXCL9. Mice infected with MHV-cCXCL9 exhibited increased mortality rates with ~65% of infected mice dead by day 9 p.i. while 100% of MHV-CXCL9-infected mice remained alive until day 21 p.i. Data are representative of two separate experiments with a minimum of 7 mice per experimental group. (B) Viral titers are reduced (*$p \leq 0.05$) within the brains and livers of *CXCL9*−/− mice infected with MHV-CXCL9 compared to MHV-cCXCL9 at days 3, 5, and 7 p.i. By day 12 p.i., CXCL9−/− mice infected with either MHV-CXCL9 or MHV-cCXCL9 were able to reduce viral titers below detectable levels (~100 PFU/g tissue) within the brain and liver. Data are presented as average±SEM from two separate experiments with a minimum of three mice per time point.

CXCL9-infected mice was associated with accelerated reduction in viral burden within both brain and liver compared to MHV-cCXCL9-infected animals (Fig. 6B). *CXCL9*−/− mice (Park et al., 2002) were infected with MHV-CXCL9 to determine if CXCL9 derived from the viral genome resulted in protection from disease. As shown in Fig. 7A, i.c. inoculation with MHV-CXCL9 resulted in 100% survival out to day 21 p.i. while infection with MHV-cCXCL9 resulted in ~65% survival. Correlating with survival in MHV-CXCL9-infected mice was a pronounced ability to control viral replication that coincided with accelerated reduction in viral burden within both the brain and liver when compared to mice infected with MHV-cCXCL9. Within the brains of mice infected with MHV-CXCL9, there was a significant ($p \leq 0.005$) reduction in viral titers at days 3, 5, and 7 p.i. compared to MHV-cCXCL9-infected mice (Fig. 7B). Similarly, viral titers were significantly ($p \leq 0.005$) reduced within the livers of MHV-CXCL9-infected mice compared to MHV-cCXCL9-infected mice at days 3 and 5 p.i. (Fig. 7B). However, it is important to emphasize that by day 12 p.i. surviving *CXCL9*−/− mice infected with MHV-cCXCL9 were ultimately able to reduce viral titers within both the brain and livers to levels comparable with mice infected with MHV-CXCL9 (Fig. 7B). Assessment of immune cell infiltration within infected tissues revealed increased ($p \leq 0.005$) levels of both CD4+ and CD8+ T cells present in the brains of MHV-CXCL9-infected *CXCL9*−/−

mice at days 3 and 7 p.i. compared to MHV-cCXCL9-infected mice yet similar numbers of T cell susbsets were present by day 12 p.i. in mice infected with either virus (Fig. 8A). Determination of T cell numbers within the livers revealed no differences in levels of infiltrating CD4+ or CD8+ T cells in *CXCL9*−/− mice infected with either MHV-CXCL9 or MHV-cCXCL9 at days 3, 7, and 12 p.i. (Fig. 8B). Infiltration of NK cells into the brains was reduced ($p \leq 0.05$) in mice infected with MHV-cCXCL9 compared to MHV-CXCL9-infected mice while there were no differences in NK cell infiltration within the livers of mice infected with either virus at any time point examined (Fig. 8C).

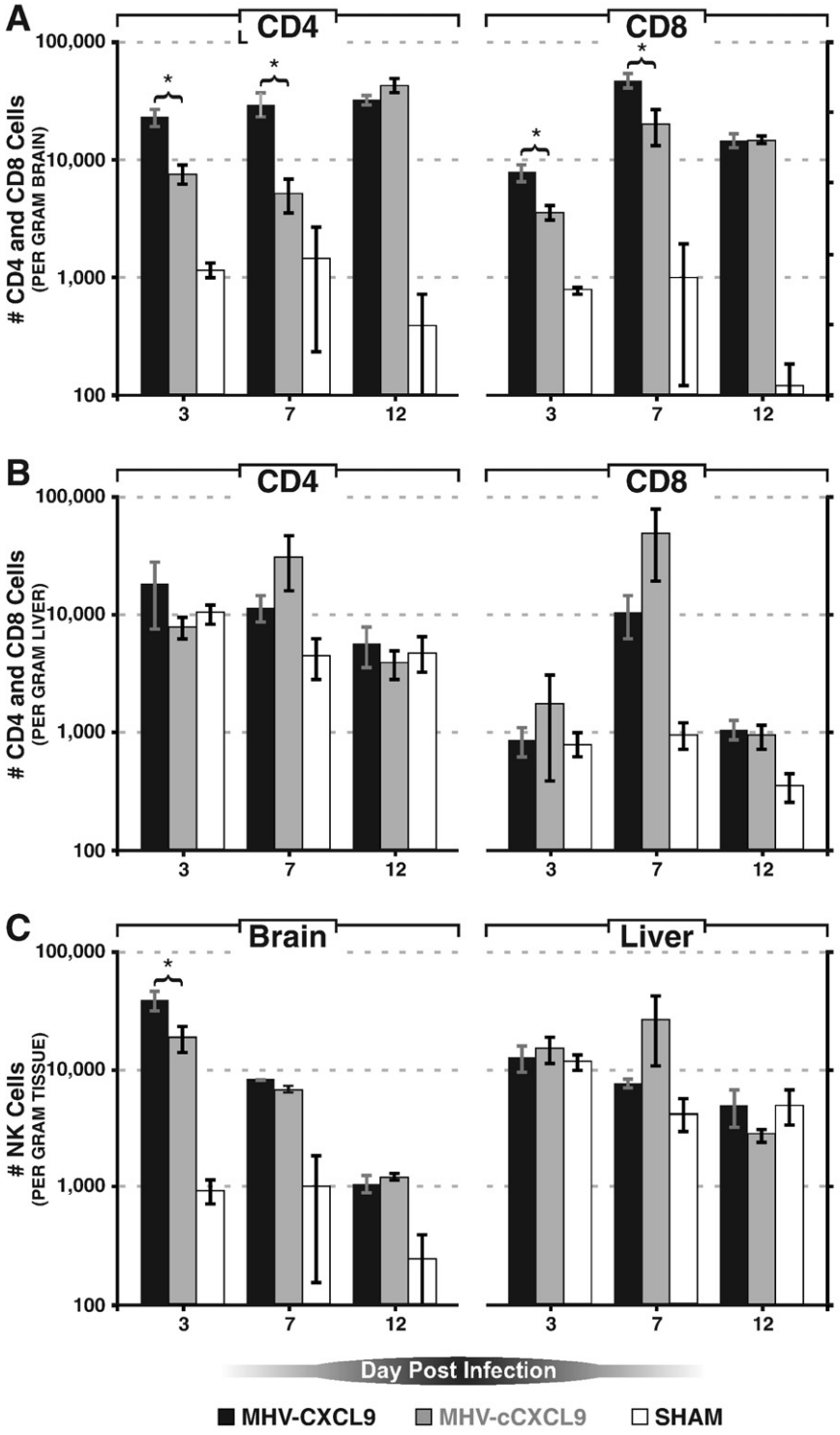

Fig. 8. T cell and NK cell infiltration into brains and livers of infected *CXCL9*−/− mice. *CXCL9*−/− mice were infected i.c. with either MHV-CXCL9 or MHV-cCXCL9 and T cell and NK cell infiltration into the brains and livers determined at indicated times p.i. (A) Infection with MHV-CXCL9 resulted in accelerated (*$p \leq 0.05$) accumulation of both CD4+ and CD8+ T cells in the brain at days 3 and 7 p.i. compared to mice infected with MHV-cCXCL9. By day 12 p.i. there was no difference in numbers of CD4+ or CD8+ T cells within the brains of mice infected with either virus. (B) No differences were detected in either CD4+ or CD8+ T cell migration into the livers of mice infected with MHV-CXCL9 compared to MHV-cCXCL9 at any time point examined. (C) NK cell infiltration was increased (*$p \leq 0.05$) within the brains of MHV-CXCL9-infected mice at day 3 p.i. compared to mice infected with MHV-cCXCL9 yet similar numbers of NK cells were present at days 7 and 12 p.i. in mice infected with either virus. No differences in NK cell infiltration within the livers were detected in mice infected with either MHV-CXCL9 of MHV-cCXCL9. Data are presented as average±SEM from two separate experiments with a minimum of three mice per time point.

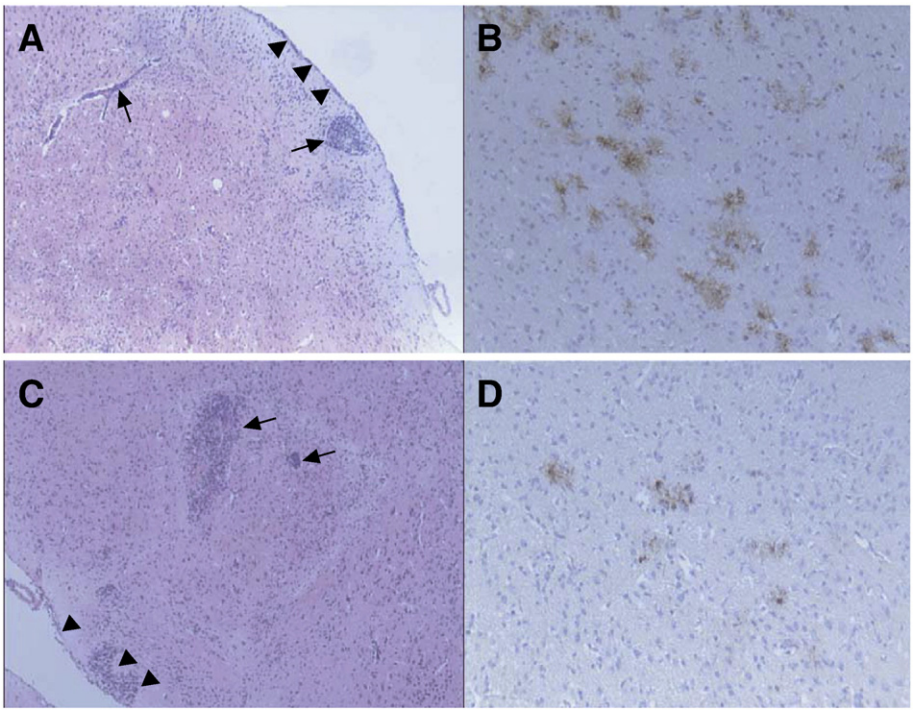

Fig. 9. Histopathology of brains from infected *CXCL9*−/− mice. Representative brain and sections from *CXCL9*−/− mice infected with either MHV-cCXCL9 or MHV-CXCL9 at day 7 p.i. Brains from MHV-CXCL9-infected mice (C) exhibited large perivascular infiltrates (arrows) and meningeal inflammatory lesions (arrowheads) when compared to mice infected with MHV-cCXCL9 (A). Staining for viral antigen revealed numerous infected cells within the hippocampus of MHV-cCXCL9-infected mice (B) compared to mice infected with MHV-CXCL9 (D). Histology and antigen staining was performed for two separate experiments with 2 mice per group and a minimum of 6 sections per mouse examined. Panels A and C, 40× magnification and panels B and D, 400× magnification.

Histological analysis of brains of mice infected with MHV-CXCL9 at day 7 p.i. demonstrated an overall increase in inflammatory cell infiltration with leukocyte accumulation within the perivasculature as well as meningeal inflammation (Fig. 9C) compared to mice infected with MHV-cCXCL9 (Fig. 9A). Immunostaining for MHV in the brains of MHV-CXCL9-infected mice supported the titer data with far fewer cells staining positive for viral antigen (Fig. 9D) when compared to the brains of MHV-cCXCL9-infected mice which had extensive staining for virus (Fig. 9B). Examination of the spinal cords of surviving mice indicated overall similar severity of white matter damage in mice infected with either MHV-CXCL9 or MHV-cCXCL9 (data not shown). Livers from mice infected with MHV-CXCL9 at day 5 p.i. exhibited small and scattered foci of periportal inflammation consisting mostly of lymphocytes and vascular congestion (Fig. 10D). In contrast, MHV-cCXCL9 infection resulted in a more pronounced and severe hepatitis with portal tracts destroyed by a combination of necrotic hepatocytes, neutrophils, and lymphocytes (Fig. 10A). In correlation with the viral titer data, there was decreased viral antigen detected in the livers of *CXCL9*−/− mice infected with MHV-CXCL9 (Figs. 10E, F) compared to MHV-cCXCL9 (Figs. 10B, C) infection. In both experimental groups, viral antigen was present in hepatocytes encircling areas of focally necrotic regions although this was dramatically reduced within MHV-CXCL9-infected mice. In addition, MHV-cCXCL9-infected mice exhibited significantly increased ($p \leq 0.01$) levels of serum alanine transferase (sALT) within the blood compared to MHV-CXCL9-infected mice, further supporting increased liver disease in MHV-cCXCL9-infected mice (Fig. 10G).

Discussion

This study utilized a reverse genetics approach to insert the chemokine CXCL9 coding sequence into the genome of MHV in order to characterize how CXCL9 may influence host defense and/or disease in response to MHV infection. The results presented support and extend earlier studies demonstrating a role for CXCL9 in host defense in response to MHV infection (Liu et al., 2001). In these experiments, administration of blocking antibodies specific for CXCL9 to mice infected with the neurotropic JHM strain of MHV (JHMV), resulted in increased mortality that correlated with diminished T cell infiltration into the CNS and correspondingly higher viral titers. The present study demonstrated that infection of mice in which CXCL9 is genetically silenced with the *A59* strain of MHV, which is capable of replicating in both brain and liver, results in rapid mortality presumably due to inability to sufficiently control viral replication in target organs. CXCL9 is expressed in both brain and liver early following MHV-A9 infection of both C57BL/6 and *RAG1*−/− mice emphasizing that this chemokine is rapidly secreted in response to infection. However, infected *RAG1*−/− mice displayed a similar mortality curve as infected *CXCL9*−/− mice and these findings demonstrate the importance of infiltrating leukocytes in controlling MHV replication within these tissues. Our findings highlight a previously unappreciated role for CXCL9 in enhancing innate immune responses as MHV-CXCL9 infection of *RAG1*−/− mice resulted in prolonged survival that correlated with reduced viral titers in both brain and liver when compared to *RAG1*−/− mice infected with MHV-cCXCL9. Increased NK cell infiltration into the liver, but not the brain, was observed in MHV-CXCL9-infected mice compared to mice infected with the control MHV-cCXCL9 virus. Furthermore, depletion of NK cells from MHV-CXCL9-infected *RAG1*−/− mice resulted in increased viral titers within the livers, but not the brains, indicating that NK cells contribute in controlling MHV replication within the liver but are dispensable in host defense within the CNS. These findings support earlier studies demonstrating an important role for NK cells in controlling MHV replication within the liver (Walsh et al., 2007; Walsh et al., 2008). These findings are also of interest as we have previously determined that i.c. infection of *RAG1*−/− mice with a recombinant MHV expressing CXCL10 (MHV-CXCL10) resulted in increased survival accompanied by reduced viral titers that correlated

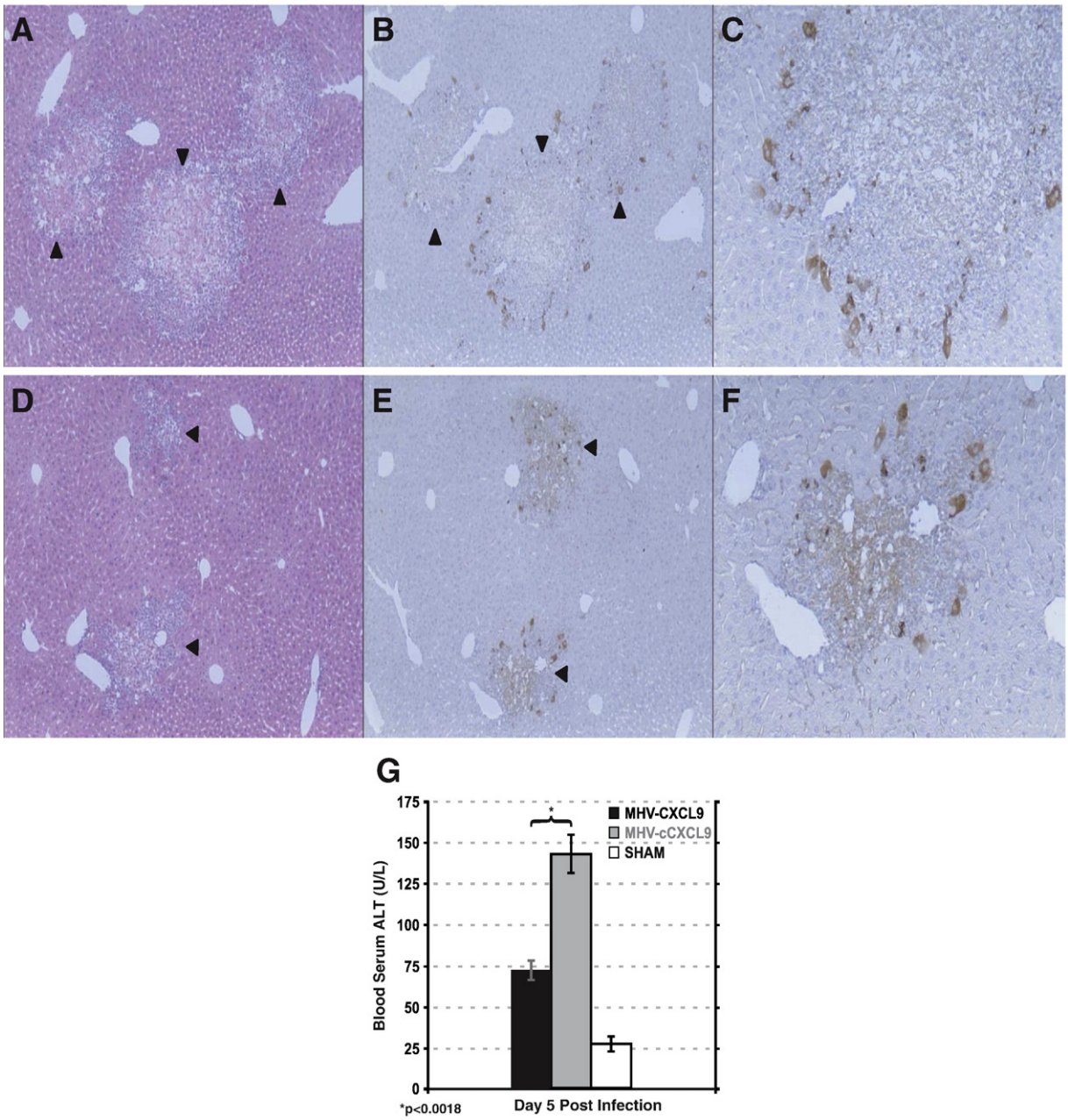

Fig. 10. Liver pathology following viral infection of *CXCL9*−/− mice. Livers from MHV-CXCL9-infected mice (D) displayed fewer foci of inflammation (arrowheads) while livers from MHV-cCXCL9-infected mice (A) exhibited more severe hepatitis with concentric rings of necrotic hepatocytes mixed with a predominant lymphocyte and neutrophil infiltrate. Histology was performed for two separate experiments with 2 mice per group and a minimum of 6 sections per mouse examined. Viral antigen was detected within hepatocytes encircling hepatic lesions (arrowheads) of mice infected with either MHV-CXCL9 (E) or MHV-cCXCL9 (B). Infection resulted in viral antigen in hepatocytes encircling areas of focally necrotic regions in MHV-CXCL9 (F) and MHV-cCXCL9 (C) infected mice. Immunostaining was performed for two separate experiments with a minimum of 2 mice per group with 6 sections per mouse examined. (G) sALT data are representative of 2 separate experiments and no fewer than 2 mice per group. Panels A, B, D, and E, 100× magnification; panels C and F, 400× magnification.

with elevated NK cell infiltration into the CNS and IFN-γ expression (Trifilo et al., 2004). Depletion of NK cells in MHV-CXCL10-infected *RAG1*−/− mice resulted in increased viral burden in the brain indicating that increased expression of CXCL10 within the CNS mice lacking a functional adaptive immune response conferred protection via attraction of NK cells (Trifilo et al., 2004). These findings are also supported by earlier studies by Mahalingam and colleagues (Mahalingam et al., 1999) in which infection of athymic nude mice with recombinant vaccinia viruses expressing either CXCL9 or CXCL10 resulted in protection from disease that was mediated by IFN-γ production by NK cells. In contrast, the data presented in this study highlights functional differences with regards to CXCL9 expression and host defense within the CNS of *RAG1*−/− mice infected with MHV with regards to NK cells. Although MHV-CXCL9-infected *RAG1*−/− mice exhibited increased survival that correlated with a reduction in viral titers within the brains, protection from CNS disease was not associated with increased NK cell infiltration or IFN-γ production and depletion of NK cells did not result in increased viral titers. Therefore, these findings argue that protection mediated by inclusion of CXCL9 into the MHV genome is separate from either attracting and/or activating NK cells and suggest alternative mechanisms to control viral replication. Whether viral-derived CXCL9 increases local type I IFN expression within the CNS that is capable of dampening MHV replication (Ireland et al., 2008) or mutes MHV receptor expression by susceptible cells which limits the spread of virus remains to be determined. Alternatively, it may also be possible that increased levels

of CXCL9 may inhibit viral binding to target cells through binding to heparin sulfate on the cell surface as Chen and colleagues (Chen et al., 2006) have recently reported that CXCL10 interaction with heparin sulfate inhibits Dengue virus from binding target cells.

Infection of C57BL/6 mice with MHV-CXCL9 resulted in increased protection from disease that correlated with accelerated clearance of virus from both brain and liver when compared to mice infected with MHV-cCXCL9 and this most likely correlates with increased T cell infiltration into target tissues in response to elevated CXCL9 production from the virus. However, surviving mice infected with MHV-cCXCL9 were eventually able to clear virus below levels of detection. In order to more accurately define mechanisms associated with CXCL9-mediated protection, *CXCL9*−/− mice were infected with the recombinant viruses. Infection with MHV-CXCL9 resulted in increased survival associated with increased infiltration of both CD4+ and CD8+ T cells into the CNS and a corresponding decrease in viral burden. These findings are consistent with earlier studies from our laboratory indicating that antibody targeting of CXCL9 following MHV infection of the CNS resulted in increased mortality as a result of decreased T cell accumulation within the CNS indicating CXCL9 can function in host defense by attracting T cells into the CNS in response to MHV infection (Liu et al., 2001). Correspondingly, increased mortality accompanied by reduced T cell infiltration into the CNS was observed in CXCL9 deficient mice infected with MHV-cCXCL9. However, it is important to emphasize that MHV-cCXCL9 infection of *CXCL9*−/− mice did not result in 100% mortality while infection with wild type MHV-A59 did kill 100% of mice. At this time, the underlying mechanisms responsible for this difference are not defined as infection of RAG1−/− with MHV-cCXCL9 resulted in a similar mortality curve as MHV-A59. This difference may relate to potentially reduced rate of spread/replication of MHV-cCXCL9 within infected tissues compared to MHV-A59. Nevertheless, we believe this doesn't diminish the strengths of the model system employed nor detract from the importance of CXCL9 in host defense following MHV infection. With regards to MHV-cCXCL9 infection of C57BL/6 and CXCL9−/− mice, increased survival supports the possibility that other chemokines, notably CXCL10 and CCL5, are likely to compensate and aid in attracting virus-specific T cells into the CNS (Glass et al., 2004; Liu et al., 2001b). We do not believe that the absence of CXCL9 impairs the generation of virus-specific T cells following MHV infection as similar numbers of T cells specific for MHV are generated in either *CXCL9*−/− or *CXCL9*+/+ mice in response to MHV infection (data not shown). Moreover, there were no detectable differences in the ability of leukocytes to exit the microvasculature and enter the parenchyma in *CXCL9*−/− mice infected with either MHV-CXCL9 or MHV-cCXCL9 indicating that the absence of CXCL9 did not affects positional migration of cells following migration to the CNS. Therefore, we conclude that viral-derived CXCL9 aids in protection from MHV-induced encephalitis by attracting CXCR3-positive T cells to sites of infection. Park et al. (Park et al., 2002) have reported increased susceptibility of *CXCL9*−/− mice to bacterial infections and also suggest that CXCL9 expression serves to optimize antibody production through facilitating interactions between lymphocytes and antigen presenting cells within secondary lymphatic tissues. Although we did not examine MHV-specific antibody production following infection of *CXCL9*−/− mice, we don't believe that lack of CXCL9 expression altered a protective humoral response as there was no viral recrudescence within spinal cords nor increase in mortality during later stages of disease in mice infected with MHV-which is associated with deficiencies in antibody production (Ramakrishna et al., 2002, 2003). Examination of spinal cords of mice infected with either MHV-CXCL9 or MHV-cCXCL9 indicate no differences in the severity of demyelination supporting earlier studies that CXCL9 expression does not significantly influence white matter damage in mice persistently infected with MHV (Liu et al., 2001b).

Previous studies have demonstrated that CXCL9 is associated with protection in response to viral infection of the liver (Arai et al., 2002; Hokeness et al., 2007; Kakimi et al., 2001a, 2001b; Salazar-Mather et al., 2000). Indeed, administration of blocking antibodies specific for CXCL9 to mice infected with various hepatotropic viral pathogens results in alterations in liver pathology that is associated with a modulation in leukocyte recruitment and highlight the importance of CXCL9 in attracting activated CXCR3-bearing inflammatory cells (Arai et al., 2002; Hokeness et al., 2007; Kakimi et al., 2001a, 2001b; Salazar-Mather et al., 2000). Through use of mice deficient in CXCL9, our studies support and extend these earlier observations and indicate an important role for CXCL9 in promoting a protective response following MHV infection of the liver. However, protection afforded by CXCL9 was not associated with any sustained increase in T cells or NK cells within the livers indicating that CXCL9 exerts a protective effect independent of enhanced recruitment of inflammatory cells. This finding is consistent with an earlier report from our laboratory demonstrating that infection of *CXCL10*−/− mice with MHV-CXCL10 results in reduced viral titers within the livers and protection from hepatitis but is not associated with increased T cell or NK cell infiltration (Walsh et al., 2007). Signaling through NKG2D has been shown to participate in control of JHMV replication within the livers yet the mechanisms *e.g.* enhanced cytokine secretion and/or cytolytic activity by inflammatory cells has yet to be defined (Walsh et al., 2008). The mechanisms by which both CXCL9 and CXCL10 promote a protective response in the liver following MHV infection independent of enhancing immune cell infiltration is the focus of ongoing investigations.

Materials and methods

Viruses and cells

All stocks of MHV-A59 mutants and recombinants were propagated in mouse 17CL1 cells and plaque titrations were carried out with mouse L2 cells. For the determination of single-step growth kinetics, monolayers of 17CL1 cells (100 cm^2) were inoculated with MHV-CXCL9 or MHV-cCXCL9 at a multiplicity of 0.01 PFU per cell for 2 h at 37 °C with rocking every 15 min. Inocula were removed, monolayers were thoroughly rinsed with 37 °C HBSS and media (DMEM, 10% FBS) was replaced. Incubation was continued at 37 °C and aliquots of media were withdrawn at 1, 3, 6, 9, 12, 24 and 48 h post infection: infectious titers were subsequently determined. All viral titer assays were performed using DBT monolayers as previously described (Glass et al., 2001).

Mice

Age-matched 5–7 week old C57BL/6 mice and *RAG1*−/− (H-2^b background) were purchased from the National Cancer Institute, Bethesda, MD. In addition, *CXCL9*−/− mice (C57BL/6, H-2b background, Park et al., 2002) were bred in the UCI vivarium and 5–7 week old mice used for experiments. Following anesthetization by i.p. injection with ketamine, mice were injected i.c. with virus (5000 PFU) suspended in 30 μl of sterile saline. Experiments for all animal studies described have been reviewed and approved by an appropriate institutional review committee.

Plasmid constructs

A transcription vector for the construction of a CXCL9-expressing recombinant virus was derived from plasmid pMH54 (Kuo et al., 2000). In brief, pMH54 contains the bacteriophage T7 RNA polymerase promoter and a cDNA copy of the 5′-most 0.5 kb of the MHV genome fused to the 3′-most 8.6 kb of the MHV genome. The MHV sequence corresponds exactly to that of wild-type MHV-A59, with the exception that it encodes silent AvrII and AseI sites [introduced into the S protein open reading frame (ORF)] and three additional nucleotides that result in the creation of an Sse8387I restriction site

12 bp downstream of the S ORF) (Kuo et al., 2000). The three nucleotide addition results in an up-regulation of subgenomic mRNA4 synthesis for reasons that are not currently understood. For construction of plasmid pMH54-CXCL9, the CXCL9 ORF was cloned from cDNA derived from mouse brain mRNA obtained from an MHV-infected mouse at day 7 post-infection (p.i.) using CXCL9-specific primers. This construct (designated WT-CXCL9-1) was cloned into Stratagene's pPCR-Script Amp SK (+) cloning vector (San Diego, CA) and served as the template for the two PCR reactions that yielded i) CXCL9-MHV [CXCL9 coding sequence (CDS)] and ii) cCXCL9-MHV (inverted CXCL9 CDS with engineered stop codons). CXCL9-MHV and cCXCL9-MHV were each ligated into the pPCR-Script cloning vector and the resulting plasmid vectors were transformed into *E. coli*, grown to high concentrations, and subsequently purified using Midiprep Kits (Qiagen, Valencia CA). The inserts were released from specific plasmid vectors by cutting with the Sse8387I and BspE1 restriction endonucleases and gel purified fragments subsequently ligated into the pMH54 vector resulting in generation of pMH54-CXCL9 (wild type CXCL9 construct containing CXCL9-MHV insert) and pMH54-cCXCL9 (control construct containing inverted CXCL9 CDS with stop codons) (Fig. 2A). These plasmids were transformed into *E. coli* and purified plasmids pMH54/CXCL9 and pMH54/cCXCL9 were linearized with PacI restriction endonuclease and served as the templates for RNA synthesis.

RNA synthesis and viral recombination

RNA was synthesized from the linearized plasmids pMH54-CXCL9 and pMH54-cCXCL9 using a T7 RNA-polymerase based reverse transcription kit (T7 mMessage mMachine, Ambion, Austin TX). These RNAs, corresponding to the 5′ end of the MHV genome and containing either the CXCL9 or cCXCL9 transgenic coding sequences, were transfected into L2 cells that had already been infected with MHV-*Alb*4 2 h prior. MHV-*Alb*4 is a strain featuring a 29aa deletion in the *N* gene rendering the virus temperature-sensitive and thermolabile at 39 °C (Kuo et al., 2000; Masters et al., 1994). These infected and transfected cells were overlayed onto confluent monolayers of 17CL1 cells and progeny virus was collected at the first signs of cytopathic effects (usually within 24–48 h of overlay) in the 17CL1 monolayers.

Screening and analysis of putative recombinants

Screening for recombinant viruses containing either the transgenic CXCL9 or cCXCL9 sequence was performed in several steps. First, confluent L2 cell monolayers were infected with various dilutions of passage 1 progeny that was previously harvested from the 17CL1 monolayers. Dilutions of passage 1 virus stocks were incubated with the L2 monolayers for two hours (with shaking every 15 min) and after 2 h the supernatant was removed and the cells were overlayed with a 50:50 mixture of 1.9% Nobel agar and 2X DMEM. These monolayers were incubated at 39 °C for 2 days. At 39 °C non-recombinant temperature sensitive MHV-*Alb*4 will form small plaques (1–2 mm) whereas recombinant progeny are easily distinguished by a much larger (4–5 mm) plaque-size. Several putative recombinant progeny plaques were isolated for each viral construct and purified by two rounds of plaque titration. Monolayers of 17CL1 cells were infected with these putative recombinants and RNA was purified from these infected monolayers at the first signs of CPE using Ultraspec reagent (Biotecx Laboratories, Houston TX). cDNAs were synthesized from these RNAs and the targeted insertion-regions were cloned and sequenced from each isolate. Progeny virus with the correct nucleotide sequence were thereafter named MHV-CXCL9 (WT-CXCL9 sequence) and MHV-cCXCL9 (control/inverted CXCL9 sequence with stop-codons) and grown over two passages in serum-free media.

Mononuclear cell isolation and flow cytometry

Immunophenotyping of the cellular infiltrate present within either brains and livers of infected mice was accomplished by homogenized isolated tissue and generating a single cell suspension and characterizing by flow cytometry. Cell suspensions were transferred to 15-mL conical tubes and Percoll (Pharmacia, Uppsala, Sweden) was added for a final concentration of 30%. One milliliter of 70% Percoll was underlaid, and the cells were centrifuged at 1300×*g* for 30 min at 4 °C. Cells were removed from the interface and washed twice. Livers were diced with a razor blade and a single cell suspension was layered over an equal volume of Lympholyte M (Cedar Lane, Ontario, Canada) in a 15 mL conical tube and centrifuged at 1250×*g* for 20 min at 4 °C. Cells were removed from the interface and washed twice. FITC-conjugated rat anti-mouse NK1.1 (BD PharMingen, San Diego, CA), FITC-conjugated rat anti-mouse CD8a for $CD8^+$ T cells (BD Pharmingen, San Diego, CA); APC-conjugated rat anti-mouse CD4 (BD Pharmingen, San Diego, CA) for $CD4^+$ T cells were was used to immunophenotype infiltrating cells. As controls, isotype-matched FITC and APC Abs were used. Cells were incubated with Abs for 30 min at 4 °C, washed, and analyzed on a FACStar (BD Biosciences, Mountain View, CA). Data are presented as the total number of positive cells within the gated population of cells from the isolated tissue.

NK cell depletion

RAG1−/− mice were infected with MHV-CXCL9 and treated with 0.5 mg of anti-asialo GM1 antisera (Wako Chemicals, Richmond, VA) or sterile HBSS (control) by intraperitoneal (i.p.) injection on days -1, 0, 1 and 3 p.i. and NK cell infiltration into brains and livers determined.

Pathology and immunohistochemistry

Brains and livers were removed at day 5 p.i. and placed in 5 mL of Formal-Fixx™ (ThermoShandon, Pittsburg, PA) overnight at room temperature after which portions of tissue were embedded in paraffin. Distribution of viral antigen was determined by immunoperoxidase staining (Vectastain-ABC kit; Vector Laboratories, Burlingame, CA) using the anti-JHMV mAb J.3.3 specific for the carboxyl terminus of the viral nucleocapsid protein as a primary antibody and horse anti-mouse IgG secondary antibody (Vector Laboratories, Burlingame, CA) (Walsh et al., 2007b). Serum alanine aminotransferase (sALT) concentrations were determined by using Infinity™ ALT (GPT) Liquid Stable Reagent (Thermo, Noble Park, Victoria, Australia) according to manufacturer's specifications.

ELISA

Assessment of CXCL9 in the supernatants of MHV-CXCL9- and MHV-cCXCL9-infected cells was determined with mouse MIG (CXCL9) ELISA kit (R&D Systems, Minneapolis, MN) according to manufacturer specifications. The results are presented as pg/mL.

Statistical analysis

All data were analyzed by performing the Student's *t*-test using Sigma-Stat 2.0 software. Values of $p \leq 0.05$ were considered significant.

Acknowledgments

The authors gratefully acknowledge Robert Edwards for his assistance in evaluating tissue pathology and Lucia Whitman for her technical assistance.

References

Arai, K., Liu, Z.X., Lane, T., Dennert, G., 2002. IP-10 and Mig facilitate accumulation of T cells in the virus-infected liver. Cell. Immunol. 219 (1), 48–56.

Bergmann, C.C., Lane, T.E., Stohlman, S.A., 2006. Coronavirus infection of the central nervous system: host-virus stand-off. Nat. Rev. Microbiol. 4 (2), 121–132.

Chen, B.P., Kuziel, W.A., Lane, T.E., 2001. Lack of CCR2 results in increased mortality and impaired leukocyte activation and trafficking following infection of the central nervous system with a neurotropic coronavirus. J. Immunol. 167 (8), 4585–4592.

Chen, J.P., Lu, H.L., Lai, S.L., Campanella, G.S., Sung, J.M., Lu, M.Y., Wu-Hsieh, B.A., Lin, Y.L., Lane, T.E., Luster, A.D., Liao, F., 2006. Dengue virus induces expression of CXC chemokine ligand 10/IFN-gamma-inducible protein 10, which competitively inhibits viral binding to cell surface heparan sulfate. J. Immunol. 177 (5), 3185–3192.

Dufour, J.H., Dziejman, M., Liu, M.T., Leung, J.H., Lane, T.E., Luster, A.D., 2002. IFN-gamma-inducible protein 10 (IP-10; CXCL10)-deficient mice reveal a role for IP-10 in effector T cell generation and trafficking. J. Immunol. 168 (7), 3195–3204.

Farber, J.M., 1997. Mig and IP-10: CXC chemokines that target lymphocytes. J. Leukoc. Biol. 61 (3), 246–257.

Glass, W.G., Liu, M.T., Kuziel, W.A., Lane, T.E., 2001. Reduced macrophage infiltration and demyelination in mice lacking the chemokine receptor CCR5 following infection with a neurotropic coronavirus. Virology 288 (1), 8–17.

Glass, W.G., Chen, B.P., Liu, M.T., Lane, T.E., 2002. Mouse hepatitis virus infection of the central nervous system: chemokine-mediated regulation of host defense and disease. Viral Immunol. 15 (2), 261–272.

Glass, W.G., Hickey, M.J., Hardison, J.L., Liu, M.T., Manning, J.E., Lane, T.E., 2004. Antibody targeting of the CC chemokine ligand 5 results in diminished leukocyte infiltration into the central nervous system and reduced neurologic disease in a viral model of multiple sclerosis. J. Immunol. 172 (7), 4018–4025.

Ho, H.H., Ivashkiv, L.B., 2006. Role of STAT3 in type I interferon responses. Negative regulation of STAT1-dependent inflammatory gene activation. J. Biol. Chem. 281 (20), 14111–14118.

Hokeness, K.L., Deweerd, E.S., Munks, M.W., Lewis, C.A., Gladue, R.P., Salazar-Mather, T.P., 2007. CXCR3-dependent recruitment of antigen-specific T lymphocytes to the liver during murine cytomegalovirus infection. J. Virol. 81 (3), 1241–1250.

Ireland, D.D., Stohlman, S.A., Hinton, D.R., Atkinson, R., Bergmann, C.C., 2008. Type I interferons are essential in controlling neurotropic coronavirus infection irrespective of functional CD8 T cells. J. Virol. 82 (1), 300–310.

Kakimi, K., Lane, T.E., Chisari, F.V., Guidotti, L.G., 2001a. Cutting edge: inhibition of hepatitis B virus replication by activated NK T cells does not require inflammatory cell recruitment to the liver. J. Immunol. 167 (12), 6701–6705.

Kakimi, K., Lane, T.E., Wieland, S., Asensio, V.C., Campbell, I.L., Chisari, F.V., Guidotti, L.G., 2001b. Blocking chemokine responsive to gamma-2/interferon (IFN)-gamma inducible protein and monokine induced by IFN-gamma activity in vivo reduces the pathogenetic but not the antiviral potential of hepatitis B virus-specific cytotoxic T lymphocytes. J. Exp. Med. 194 (12), 1755–1766.

Koetzner, C.A., Parker, M.M., Ricard, C.S., Sturman, L.S., Masters, P.S., 1992. Repair and mutagenesis of the genome of a deletion mutant of the coronavirus mouse hepatitis virus by targeted RNA recombination. J. Virol. 66 (4), 1841–1848.

Kuo, L., Godeke, G.J., Raamsman, M.J., Masters, P.S., Rottier, P.J., 2000. Retargeting of coronavirus by substitution of the spike glycoprotein ectodomain: crossing the host cell species barrier. J. Virol. 74 (3), 1393–1406.

Lane, T.E., Buchmeier, M.J., 1997. Murine coronavirus infection: a paradigm for virus-induced demyelinating disease. Trends Microbiol. 5 (1), 9–14.

Lane, T.E., Asensio, V.C., Yu, N., Paoletti, A.D., Campbell, I.L., Buchmeier, M.J., 1998. Dynamic regulation of alpha- and beta-chemokine expression in the central nervous system during mouse hepatitis virus-induced demyelinating disease. J. Immunol. 160 (2), 970–978.

Liu, M.T., Chen, B.P., Oertel, P., Buchmeier, M.J., Armstrong, D., Hamilton, T.A., Lane, T.E., 2000. The T cell chemoattractant IFN-inducible protein 10 is essential in host defense against viral-induced neurologic disease. J. Immunol. 165 (5), 2327–2330.

Liu, M.T., Armstrong, D., Hamilton, T.A., Lane, T.E., 2001. Expression of Mig (monokine induced by interferon-gamma) is important in T lymphocyte recruitment and host defense following viral infection of the central nervous system. J. Immunol. 166 (3), 1790–1795.

Liu, M.T., Keirstead, H.S., Lane, T.E., 2001. Neutralization of the chemokine CXCL10 reduces inflammatory cell invasion and demyelination and improves neurological function in a viral model of multiple sclerosis. J. Immunol. 167 (7), 4091–4097.

Mahalingam, S., Farber, J.M., Karupiah, G., 1999. The interferon-inducible chemokines MuMig and Crg-2 exhibit antiviral activity in vivo. J. Virol. 73 (2), 1479–1491.

Mahalingam, S., Foster, P.S., Lobigs, M., Farber, J.M., Karupiah, G., 2000. Interferon-inducible chemokines and immunity to poxvirus infections. Immunol. Rev. 177, 127–133.

Marten, N.W., Stohlman, S.A., Bergmann, C.C., 2001. MHV infection of the CNS: mechanisms of immune-mediated control. Viral Immunol. 14 (1), 1–18.

Masters, P.S., Koetzner, C.A., Kerr, C.A., Heo, Y., 1994. Optimization of targeted RNA recombination and mapping of a novel nucleocapsid gene mutation in the coronavirus mouse hepatitis virus. J. Virol. 68 (1), 328–337.

Ontiveros, E., Kuo, L., Masters, P.S., Perlman, S., 2001. Inactivation of expression of gene 4 of mouse hepatitis virus strain JHM does not affect virulence in the murine CNS. Virology 289 (2), 230–238.

Park, M.K., Amichay, D., Love, P., Wick, E., Liao, F., Grinberg, A., Rabin, R.L., Zhang, H.H., Gebeyehu, S., Wright, T.M., Iwasaki, A., Weng, Y., DeMartino, J.A., Elkins, K.L., Farber, J.M., 2002. The CXC chemokine murine monokine induced by IFN-gamma (CXC chemokine ligand 9) is made by APCs, targets lymphocytes including activated B cells, and supports antibody responses to a bacterial pathogen in vivo. J. Immunol. 169 (3), 1433–1443.

Parra, B., Hinton, D.R., Marten, N.W., Bergmann, C.C., Lin, M.T., Yang, C.S., Stohlman, S.A., 1999. IFN-gamma is required for viral clearance from central nervous system oligodendroglia. J. Immunol. 162 (3), 1641–1647.

Parra, B., Lin, M.T., Stohlman, S.A., Bergmann, C.C., Atkinson, R., Hinton, D.R., 2000. Contributions of Fas-Fas ligand interactions to the pathogenesis of mouse hepatitis virus in the central nervous system. J. Virol. 74 (5), 2447–2450.

Ramakrishna, C., Stohlman, S.A., Atkinson, R.D., Shlomchik, M.J., Bergmann, C.C., 2002. Mechanisms of central nervous system viral persistence: the critical role of antibody and B cells. J. Immunol. 168 (3), 1204–1211.

Ramakrishna, C., Bergmann, C.C., Atkinson, R., Stohlman, S.A., 2003. Control of central nervous system viral persistence by neutralizing antibody. J. Virol. 77 (8), 4670–4678.

Salazar-Mather, T.P., Hamilton, T.A., Biron, C.A., 2000. A chemokine-to-cytokine-to-chemokine cascade critical in antiviral defense. J. Clin. Invest. 105 (7), 985–993.

Stiles, L.N., Hosking, M.P., Edwards, R.A., Strieter, R.M., Lane, T.E., 2006. Differential roles for CXCR3 in CD4+ and CD8+ T cell trafficking following viral infection of the CNS. Eur. J. Immunol. 36 (3), 613–622.

Templeton, S.P., Perlman, S., 2007. Pathogenesis of acute and chronic central nervous system infection with variants of mouse hepatitis virus, strain JHM. Immunol. Res. 39 (1–3), 160–172.

Trifilo, M.J., Montalto-Morrison, C., Stiles, L.N., Hurst, K.R., Hardison, J.L., Manning, J.E., Masters, P.S., Lane, T.E., 2004. CXC chemokine ligand 10 controls viral infection in the central nervous system: evidence for a role in innate immune response through recruitment and activation of natural killer cells. J. Virol. 78 (2), 585–594.

Walsh, K.B., Edwards, R.A., Romero, K.M., Kotlajich, M.V., Stohlman, S.A., Lane, T.E., 2007. Expression of CXC chemokine ligand 10 from the mouse hepatitis virus genome results in protection from viral-induced neurological and liver disease. J. Immunol. 179 (2), 1155–1165.

Walsh, K.B., Lodoen, M.B., Edwards, R.A., Lanier, L.L., Lane, T.E., 2008. Evidence for differential roles for NKG2D receptor signaling in innate host defense against coronavirus-induced neurological and liver disease. J. Virol. 82 (6), 3021–3030.

Weiner, L.P., 1973. Pathogenesis of demyelination induced by a mouse hepatitis. Arch. Neurol. 28 (5), 298–303.

Weiss, S.R., Zoltick, P.W., Leibowitz, J.L., 1993. The *ns* 4 gene of mouse hepatitis virus (MHV), strain A 59 contains two ORFs and thus differs from *ns* 4 of the JHM and S strains. Arch. Virol. 129 (1–4), 301–309.

Yokomori, K., Lai, M.M., 1991. Mouse hepatitis virus S RNA sequence reveals that nonstructural proteins ns4 and ns5a are not essential for murine coronavirus replication. J. Virol. 65 (10), 5605–5608.